C. R. Mecanique 338 (2010) 290–303

Contents lists available at ScienceDirect

Comptes Rendus Mecanique

www.sciencedirect.com

Influence of inter-granular void ratio on monotonic and cyclic undrained shear response of sandy soils

Influence de l'indice des vides inter-granulaire sur la réponse monotone et cyclique non draine des sols sableux

M. Belkhatir [a,*], A. Arab [a], N. Della [a], H. Missoum [b], T. Schanz [c]

[a] *Civil Engineering Department, University of Chlef, BP 151, Route de Sendjes, 02000 Chlef, Algeria*
[b] *Civil Engineering Department, University of Mostaganem, Algeria*
[c] *Laboratory of Foundation Engineering, Soil and Rock Mechanics, Ruhr University of Bochum, Germany*

ARTICLE INFO

Article history:
Received 27 August 2009
Accepted after revision 1 April 2010
Available online 6 May 2010

Keywords:
Soils
Silty sand
Residual shear strength
Inter-granular void ratio
Fines
Liquefaction

Mots-clés :
Sols
Sable limoneux
Résistance au cisaillement résiduelle
Indice des vides inter-granulaire
Fines
Liquéfaction

ABSTRACT

Liquefaction of sandy soil deposits during earthquakes has been one of the most important problems in the field of geotechnical earthquake engineering. A major challenge is the assessment of the appropriate undrained shear strength of liquefied soils to be used in the study of liquefaction stability of different types of earth structures (embankments, earthdams, etc.). The objective of this laboratory investigation is to study the effect of the inter-granular void ratio on the phase transition state undrained shear strength of loose, medium dense and dense ($D_r = 12$, 50, and 90%) sand–silt soil mixtures under monotonic loading and liquefaction potential under cyclic loading. For this purpose, we considered the matrix of sand with fines as a combination of two sub-matrices: a coarser grain matrix and a finer grain matrix. Moreover, series of undrained triaxial compression tests were carried out on reconstituted saturated silty sand samples with fines contents ranging from 0 to 50%. The results show that the global void ratio does not reflect the real behaviour of the soil and the undrained shear strength at the phase transition state can be correlated to the inter-granular void ratio of the sand–silt mixtures up to 50% fines content. Indeed, it decreases linearly with further increase in the inter-granular void ratio. The results of the undrained cyclic tests confirm this tendency.

RÉSUMÉ

La liquéfaction des dépôts de sols sableux pendant les séismes a toujours été l'un des problèmes les plus importants dans le domaine de la géotechnique. Un défi important est l'évaluation de la resistance au cisaillement non drainée appropriée des sols liquéfiables à utiliser dans l'étude de la stabilité de liquéfaction de différents types d'ouvrages en terre (remblais, barrages en terre, etc.). L'objectif de ce travail expérimental est d'étudier l'effet de l'indice des vides intergranulaire sur la résistance au cisaillement non drainée mesurée en changement de phase des mélanges de sable–limon lâche, moyennement dense et dense ($D_r = 12$, 50, et 90%) sous chargement monotone et le potentiel de liquéfaction sous chargement cyclique. Pour cela, nous considérons que la matrice de sable contenant les fines est la combinaison de deux matrices : une matrice de sol grenu et une matrice de sol fin. A cet effet, une série d'essais de compression triaxiale non drainés a été effectuée

* Corresponding author.
E-mail address: abelkhatir@yahoo.com (M. Belkhatir).

1631-0721/$ – see front matter
doi:10.1016/j.crme.2010.04.002

sur des échantillons de sable limoneux saturés à des teneurs en fines variant de 0 à 50%. Les résultats montrent que l'indice des vides global ne reflète pas le comportement réel du sol et que la résistance au cisaillement non drainée mesurée en changement de phase peut être corrélée avec l'indice des vides intergranulaire des mélanges de sable–limon jusqu'à une teneur en fines de 50%. En effet, elle diminue linéairement avec l'augmentation de l'indice des vides inter-granulaire. Les résultats des essais cycliques non drainés confirment cette tendance.

1. Introduction

A destructive earthquake occurred near Chlef City, Algeria on October 10th, 1980 at 13:25:23.7 local time (12:25:23.7 GMT). Chlef city is approximately 210 km west of Algiers. The magnitude on the Richter scale, M, was 7.2, corresponding to a surface wave magnitude, Ms, of 7.3. The epicenter of the quake was located at 36.143°N and 1.413°E, 10 km east of Chlef. The focal depth of the earthquake was about 10 km, and the approximate duration was between 35 and 40 sec. The earthquake devastated the city of Chlef, population estimated at 125,000, and the nearby towns and villages. The large loss of life (reportedly 5000 to 20,000 casualties) and property was attributed to the collapse of buildings. In several places of the affected area, especially along the Chlef river banks, great masses of sandy soil were ejected on to the surface level. Major damage was caused to certain structures (earthdams, embankments, bridges, slopes and buildings).

During earthquakes, the ground shakes causing sandy soils to loose their strength and behave like a liquid. This phenomenon is called soil liquefaction and causes settlement of buildings, landslides, failures of earth dams, or other hazards. Liquefaction is due to an increase in the excess pore water pressure and a corresponding decrease in the effective overburden stress in a soil deposit. The understanding of liquefaction phenomena has significantly improved in recent years. Most liquefaction research has been carried out on clean sands under the assumption that the behaviour of silty sand is similar to that of clean sands.

Recent research into the nature of soil structure and its mechanical stress-strain response indicates that the soil behaves as a collection of scale-level-dependent skeletons arranged in a particular manner (Thevanayagam [1]; Thevanayagam and Nesarajah [2]). However, many researchers have mentioned that the physical nature of silty sand is entirely different from clean sand (Zlatovic and Ishihara [3]; Lade and Yamamuro [4]; Thevanayagam et al. [5]; Thevanayagam [6]; Yamamuro and Lade [7]; Amini and Qi [8]; Naeini [9]; Naeini and Baziar [10]). They have recognized that the undrained shear strength (S_{us}) response depends effectively on the void ratio as a state parameter. It is also anticipated that the global void ratio (e) cannot represent the amount of particle contacts in the sand–silt soil sample mixture. As the void ratio and the proportion of coarse-grained and fine-grained soil change, the nature of their microstructures also changes. Due to a large grain-size distribution range and availability of voids larger than some grains, at low fines contents, some of the finer grains may remain inactive and swim in the void spaces without affecting or contributing to the force chain. Therefore, it is quite important to use new index parameters such as the inter-granular (Thevanayagam [6]; Chu and Leong [11]; Monkul [12]) and inter-fine (Naeini and Baziar [10]) void ratios to assess the undrained residual shear strength response of sand–silt mixtures. Further investigations of the microstructure of soils including two sub-matrices (i.e. coarse-grain and fine-grain matrices) are therefore needed in order to gain insight into their influence on stress-strain and compression behaviour. It may be expected that soils or reconstituted mixtures with some amount of fines content would exhibit the behaviour of the dominant grain matrix.

The results of this laboratory investigation indicate that at fines content of less than 50%, the inter-granular void ratio (e_s) plays an important role for the phase transition undrained shear strength of sand–silt mixtures. Indeed, it is shown that the undrained shear strength measured at the phase transition point can be related to the inter-granular void ratio for sand–silt mixtures with up to 50% fines content. The data also show that the undrained shear strength measured at the phase transition point decreases linearly with an increase in the inter-granular void ratio. According to the recorded data, it is reasonable to assume that the finer grains do not actively participate in the transfer of frictional contact forces, or in other words their contact force contribution is secondary. Therefore, the contribution of the fines to the force chains is minimal when the fines content is below a limit in the range of 30 to 40%, compared to higher fines contents.

2. Experimental program and test procedure

The present laboratory investigation was carried out to study the influence of inter-granular void ratio on the undrained residual shear strength of sand–silt mixtures. For this purpose, series of tests of undrained triaxial compression under monotonic loading conditions were performed on reconstituted saturated samples of Chlef sand with variations in fines content ranging from 0 to 50%. The samples were prepared to represent loose, medium dense and dense states using an undercompaction method of sample preparation and consolidated isotropically at an initial confining pressure of 100 kPa. Sand samples were collected from a liquefied layer of the deposit area close to the epicentre of the Chlef earthquake (October 10th, 1980). Fig. 1 shows craters of liquefied ground on the banks of the Chlef River. Fig. 2 illustrates typical subsidence locations of the liquefied soil and sample collection. The sand and silt used in this laboratory investigation

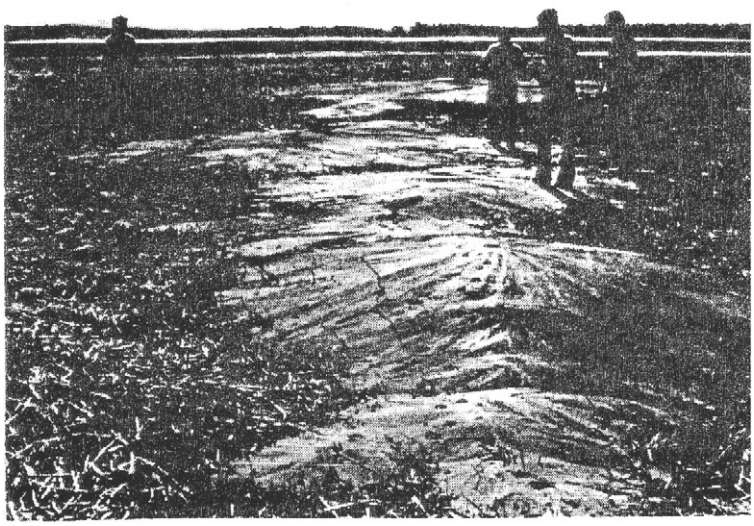

Fig. 1. Craters of liquefied ground on banks of the Chlef River.
Fig. 1. Cratères de sol liquéfié sur des banques de la rivière de Chlef.

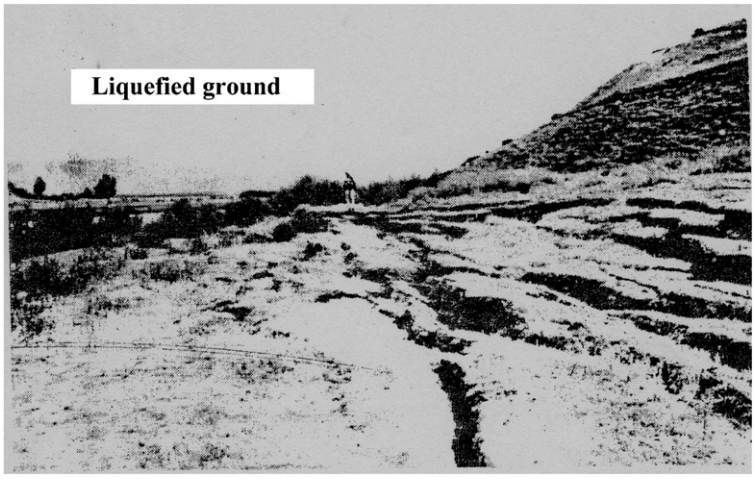

Fig. 2. Subsidence of the Chlef River banks due to liquefaction.
Fig. 2. Affaissement des banques de la rivière de Chlef due à la liquéfaction.

Table 1
Index properties of sand–silt mixtures.

Tableau 1
Propriétés physiques des mélanges sable–limon.

Material	Fines content (%)	G_S	D_{50} (mm)	C_u	$e_{\min}$	$e_{\max}$	I_p (%)
Clean sand (S100M0)	0	2.680	0.36	2.35	0.535	0.854	–
Silty sand (S90M10)	10	2.682	–	–	0.472	0.798	–
Silty sand (S80M20)	20	2.684	–	–	0.431	0.748	–
Silty sand (S70M30)	30	2.686	–	–	0.412	0.718	–
Silty sand (S60M40)	40	2.688	–	–	0.478	0.732	–
Silty sand (S50M50)	50	2.69	–	–	0.600	0.874	–
Silt (S0M100)	100	2.70	0.06	–	0.72	1.420	5.0

were obtained by dry-sieve and wet-sieve analyses. The index properties of the soils used in the study are summarized in Table 1. The grain-size distribution curves for the tested soils are shown in Fig. 3. The variation of $e_{\max}$ and $e_{\min}$ versus the fines content is illustrated in Fig. 4. Monotonic undrained compression tests were carried out on isotropically consolidated sand samples with 0, 10, 20, 30, 40 and 50% non-plastic fines. The different soil ratio samples are designated as S100M0, S90M10, S80M20, S70M30, S60M40 and S50M50, where S represents sand, M represents silt and numbers represent their

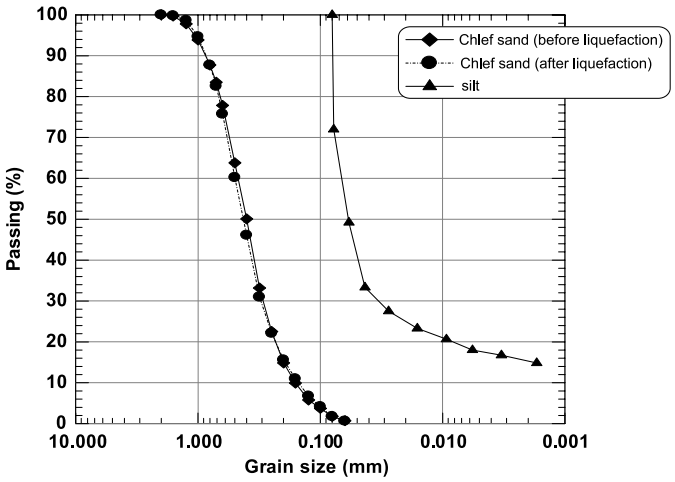

Fig. 3. Grain size distribution curves of the tested soils.

Fig. 3. Analyse granulométrique des sols testés.

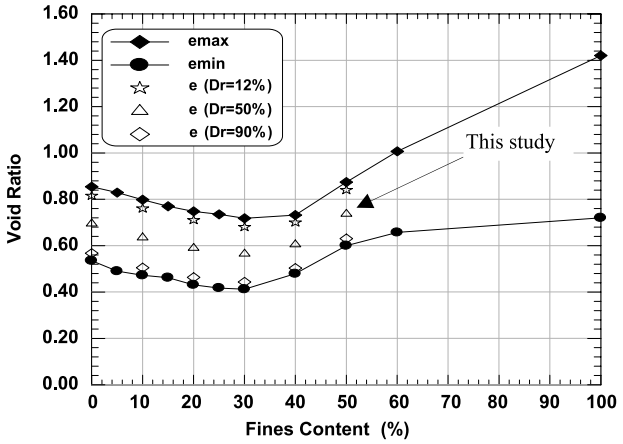

Fig. 4. Maximum and minimum void ratios of the sand–silt mixtures.

Fig. 4. Indices des vides maximal et minimal des mélanges sable–limon.

respective percentages. They were tested at an initial confining pressure of 100 kPa. All specimens were prepared by first estimating the dry weights of sand and silt needed for the desired proportion in the loose, medium dense and dense state ($D_r = 12$, 50, and 90%) using the undercompaction method of sample preparation which simulates a relatively homogeneous soil condition and is performed by compacting dry soils in layers to a selected percentage of the required dry unit weight of the specimen (Ladd [13]). The concept of undercompaction is based on the fact that when successive layers of sand are placed without undercompaction, the compaction of each succeeding layer can further densify the sand below it. In order to avoid this difficulty, the lower layers were compacted to a lower density than desired for the final density. The dry pluviation method was used to prepare samples. The specimens were 70 mm in diameter and 70 mm in height with smooth lubricated end-plates. After the specimen has been formed, the specimen cap is placed and sealed with O-rings, and a partial vacuum of 20 kPa is applied to the specimen to reduce disturbances. Saturation was performed by purging the dry specimen with carbon dioxide for approximately 30 min. De-aired water was then introduced into the specimen from the bottom drain line. Water was allowed to flow through the specimen until an amount equal to the void volume of the specimen was collected in a beaker through the specimen upper drain line. A minimum Skempton coefficient-value greater than 0.96 was obtained at a minimum back pressure of 100 kPa. All test specimens were isotropically consolidated at a mean effective pressure of 100 kPa, and then subjected to undrained monotonic triaxial loading. An advanced automated triaxial testing apparatus was used to conduct the monotonic and cyclic tests. All undrained triaxial tests for this study were carried out at constant strain rate of 0.167% per minute. The loading rate was chosen so that pore pressure equalization throughout the specimen was ensured. All the tests were continued up to 24% axial strain.

When a granular soil contains fines, the global void ratio of the soil, e, can no longer be used to describe the behaviour of the soil. This is because, up to a certain fines content, F_c (the ratio of the weight of silt to the total weight of the sand–silt

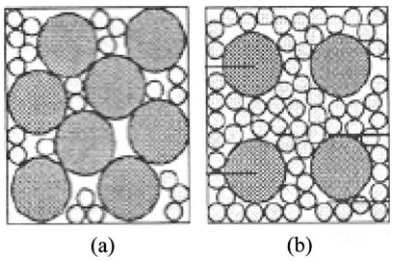

Fig. 5. Schematic diagrams representing sand–silt mixtures: (a) Coarse grains are in contact with each other, (b) coarse grains are swimming in the fines matrix.

Fig. 5. Diagramme schématique représentant les mélanges sable–limon : (a) Les gros grains sont en contacts les uns contre les autres, (b) les gros grains nagent dans la matrice des fines.

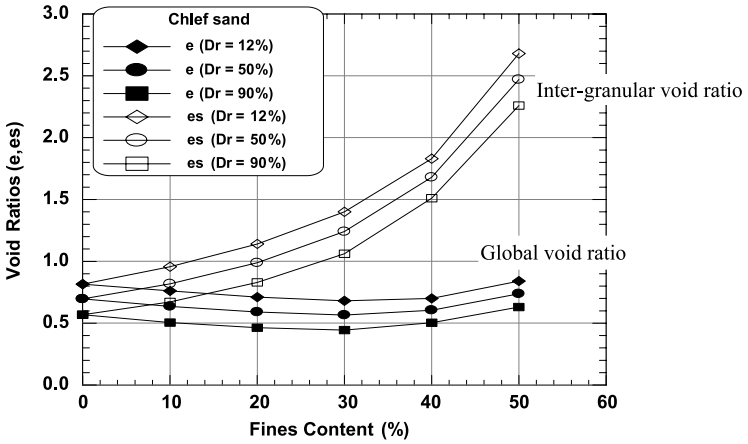

Fig. 6. Variation of void ratios with fines content.

Fig. 6. Variation des indices des vides en fonction de la teneur en fines.

mixture), the fines only occupy the void spaces, and do not significantly affect the mechanical behaviour of the sand–silt mixture. For this reason, the use of the inter-granular void ratio has been suggested (Kenny [14]; Kuerbis et al. [15]; Mitchell [16]). Mitchell [16], and later Thevanayagam and Mohan [17] proposed to consider the matrix of sand with fines as a combination of two sub-matrices: a coarse-grain matrix and a fine-grain matrix (Fig. 5). Thevanayagam and Mohan [17] also suggest that for fines content F_c (i.e. expressed as a percentage of the total weight of the soil specimen) below a limit in the range of 20 to 30%, the contribution of fines in the force chain is minimal. In this idealization, a simplifying assumption is proposed to consider the fine-grain matrix as part of the voids between the coarser grains. By neglecting the difference in the specific gravity of coarser and finer particles, an inter-granular void ratio e_s was formulated as:

$$e_s = \frac{e + (F_c/100)}{1 - (F_c/100)} \tag{1}$$

where e is the global void ratio and F_c is the fines content.

Eq. (1) gives the inter-granular void ratio as defined by Thevanayagam [6].

Fig. 6 shows the variation of void ratios versus fines content at 100 kPa mean confining pressure for the initial densities ($D_r = 12$, 50, and 90%). As shown in this figure, the global void ratio (e) decreases with the fines content until the value of 30% and then increases. However, the inter-granular void ratio (e_s) increases hyperbolically with an increase of fines content. This shows that the global void ratio cannot represent the amount of particle contacts in silty sands. As the void ratio and proportion of the coarser over the finer grains of soil change, the nature of their microstructures also changes. It is assumed in the inter-granular void ratio concept that the fines may not actively participate in sustaining the internal forces or that their contribution is secondary, if the size of the fines is too small with respect to the pore sizes of the coarse-grain matrix and the amount of fines stays within a certain margin. If the fines content is increased significantly, the soil behaviour may be completely governed by the contacts along the fines, and the coarser grains float within the fines.

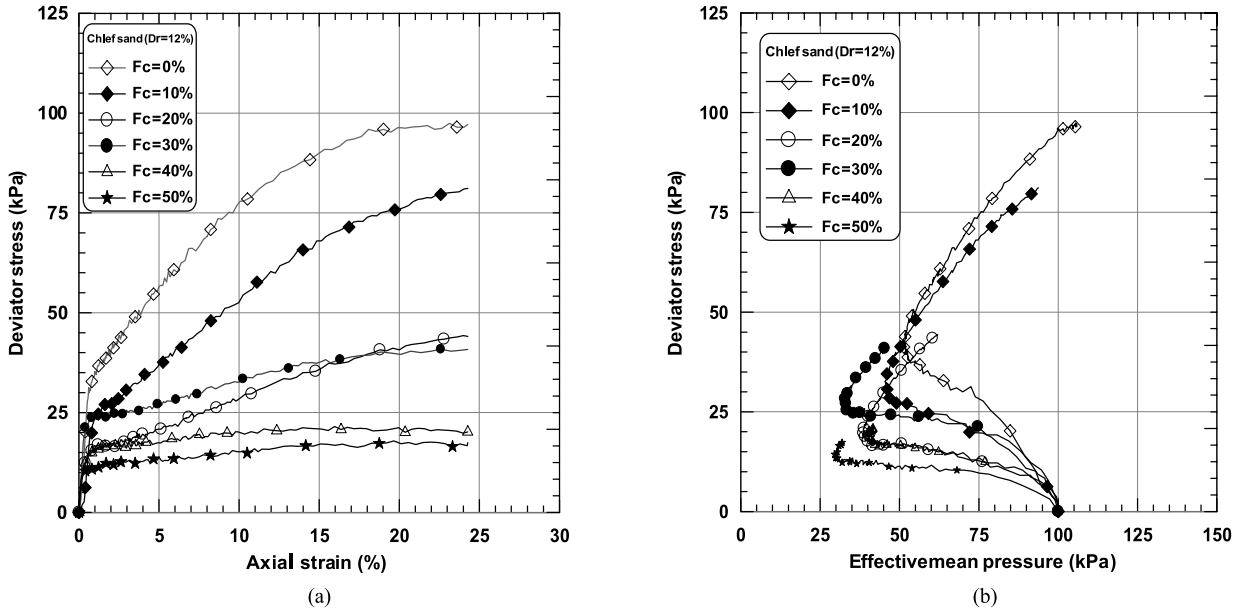

Fig. 7. Influence of the fines content on the undrained response of the sand–silt mixtures ($\sigma_3' = 100$ kPa, $D_r = 12\%$).

Fig. 7. Influence de la teneur en fines sur la réponse non drainée des mélanges sable–limon ($\sigma_3' = 100$ kPa, $D_r = 12\%$).

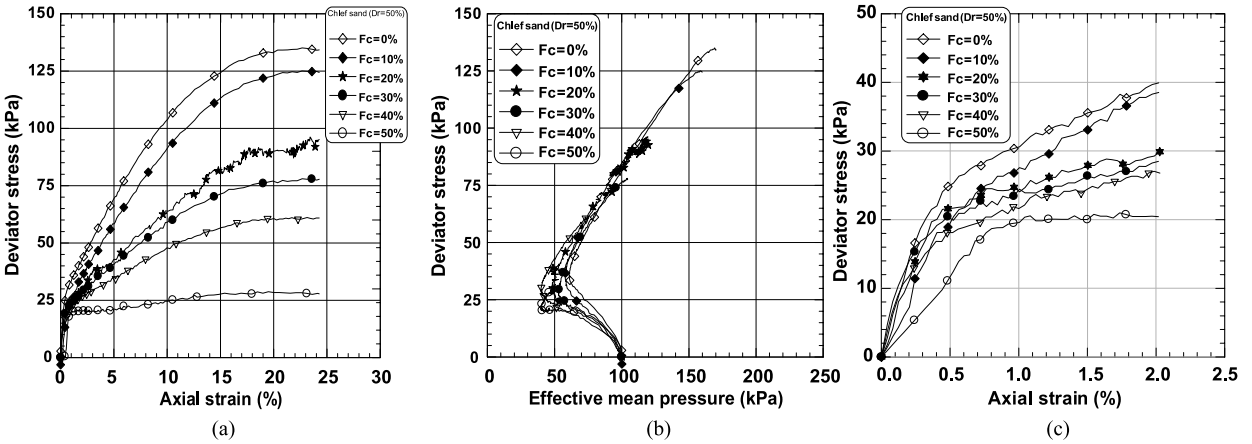

Fig. 8. Influence of the fines content on the undrained response of the sand–silt mixtures ($\sigma_3' = 100$ kPa, $D_r = 50\%$).

Fig. 8. Influence de la teneur en fines sur la réponse non drainée des mélanges sable–limon ($\sigma_3' = 100$ kPa, $D_r = 50\%$).

3. Monotonic test results

3.1. Undrained compression loading tests

Figs. 7, 8 and 9 show the results of undrained compression tests carried out for different fines content ranging from 0 to 50% at 100 kPa confining pressure for three separate densities ($D_r = 12$, 50, 90%). We notice in general that an increase in the amount of fines leads to a decrease in the deviatoric stress. The increase results from the role played by the fines in increasing the contractancy phase of the sand–silt mixtures, which leads to a reduction in the confining effective pressure and consequently to a decrease of the peak resistance of the mixtures as illustrated by Figs. 7a, 8a, and 9a. The stress path in the (p', q) plane shows clearly the role of the fines increase in the decrease of the average effective pressure and the maximum deviatoric stress (Figs. 7b, 8b and 9b). In this case, the effect of fines on the undrained behaviour of the mixtures is observed for the lower fines contents (0 and 10%), and becomes very marked beyond 20%. These results are in good agreement with the observations by Shen et al. [18] and Troncosco and Verdugo [19]. Table 2 presents the summary of the undrained monotonic tests.

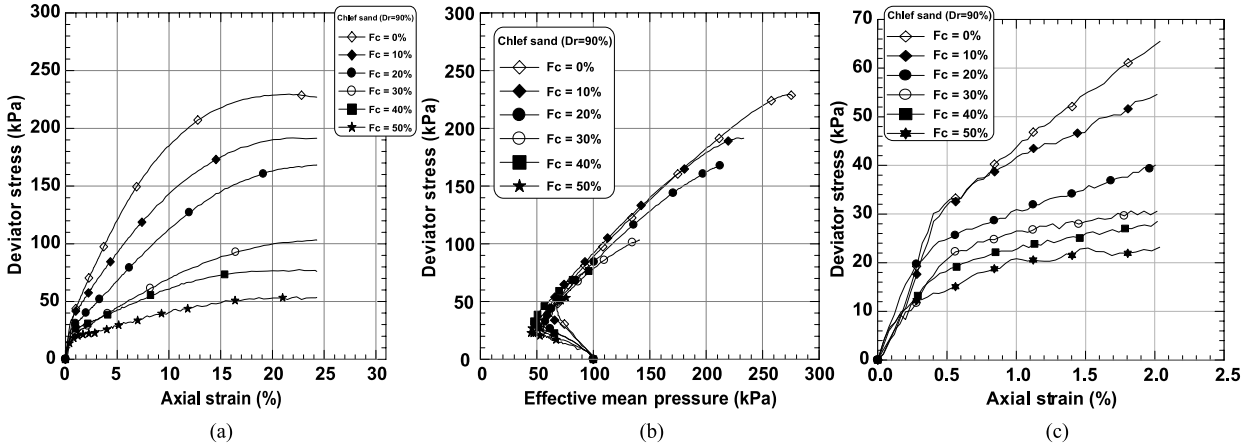

Fig. 9. Influence of the fines content on the undrained response of the sand–silt mixtures ($\sigma'_3 = 100$ kPa, $D_r = 90\%$).
Fig. 9. Influence de la teneur en fines sur la réponse non drainée des mélanges sable–limon ($\sigma'_3 = 100$ kPa, $D_r = 90\%$).

Table 2
Summary of monotonic compression triaxial tests results.

Tableau 2
Résumé des résultats des essais triaxiaux monotones.

Test no.	Materials	F_c (%)	D_r (%)	γ_d (g/cm^3)	e	e_s	S_{us} (kPa)
1	Clean sand (S100M0)		12	1.48	0.815	0.815	17.37
2		0	50	1.58	0.695	0.695	18.31
3			90	1.71	0.567	0.567	20.94
4	Silty sand (S90M10)		12	1.52	0.760	0.956	15.44
5		10	50	1.64	0.635	0.817	17.90
6			90	1.78	0.505	0.672	19.61
7	Silty sand (S80M20)		12	1.57	0.710	1.140	14.46
8		20	50	1.69	0.590	0.988	16.46
9			90	1.83	0.463	0.829	18.42
10	Silty sand (S70M30)		12	1.60	0.680	1.400	13.48
11		30	50	1.71	0.565	1.240	15.12
12			90	1.86	0.443	1.060	17.34
13	Silty sand (S60M40)		12	1.58	0.700	1.830	10.75
14		40	50	1.67	0.605	1.680	13.71
15			90	1.79	0.503	1.510	15.92
16	Silty sand (S50M50)		12	1.46	0.840	2.680	06.51
17		50	50	1.55	0.737	2.470	10.21
18			90	1.65	0.630	2.260	12.00

e = global void ratio.
e_s = inter-granular void ratio.
S_{us} = undrained shear strength at the phase transition point.

3.2. Undrained shear strength at the phase transition point

When a loose, medium dense or dense soil specimen is subjected to undrained shearing, the undrained shear strength increases rapidly until it reaches a strength point corresponding to a transitory state called contractancy–dilatancy phase change in the stress path curve (q, p'). Conventionally, this shear strength is called the undrained shear strength at the phase transition state by Ishihara [20] and the characteristics state by Luong [21]. It is defined by Ishihara [20] as

$$S_{us} = (q_s/2)\cos\phi_s = (M/2)\cos\phi_s\left(p'_s\right) \tag{2}$$

$$M = (6\sin\phi_s)/(3 - \sin\phi_s) \tag{3}$$

where q_s, p'_s and ϕ_s indicate the deviator stress $(\sigma'_1 - \sigma'_3)$, the effective mean principal stress $(\sigma'_1 + 2\sigma'_3)/3$ and the mobilized angle of inter-particle friction at the quasi-steady state (QSS) respectively. For the undrained tests conducted at the confining pressure and various initial relative densities, the deviator stress (q_s) was estimated at the phase transition point along with the mobilized friction angle. The undrained shear strength at the phase transition point was calculated with Eq. (2).

Fig. 10 illustrates the undrained shear strength measured at the phase transition point versus fines content for three densities ($D_r = 12$, 50 and 90%) at a confining pressure of 100 kPa. It is clear from this figure that the undrained shear

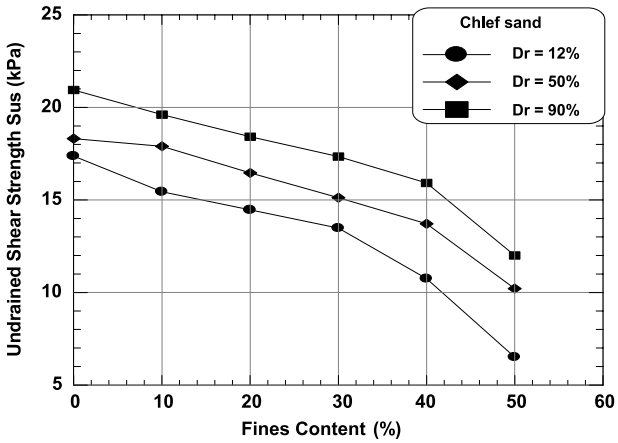

Fig. 10. Undrained shear strength at the phase transition point versus fines content ($\sigma'_3 = 100$ kPa).
Fig. 10. Résistance au cisaillement en phase transitoire en fonction de la teneur en fines ($\sigma'_3 = 100$ kPa).

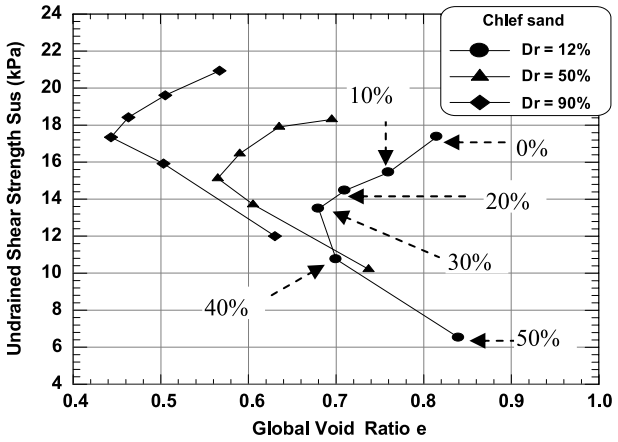

Fig. 11. Undrained shear strength at the phase transition point versus global void ratio and fines content ($\sigma'_3 = 100$ kPa).
Fig. 11. Résistance au cisaillement en phase transitoire en fonction de l'indice des vides global et teneur en fines ($\sigma'_3 = 100$ kPa).

strength at the phase transition point decreases moderately with the fines content up to the value of 40%, beyond which it decreases more sharply.

Fig. 11 shows the undrained shear strength measured at the phase transition point versus the global void ratio and fines content. It is clear from this, that the undrained shear strength at the phase transition point decreases linearly as the global void ratio (fines content) decreases for all densities ($D_r = 12$, 50, and 90%) up to 30% fines content. It means that when the global void ratio (the fines content) is decreased, the undrained shear strength at the phase transition point also decreases. This is not the case of the sand–silt mixtures, where the behaviour of silty sand soils is influenced by contacts between coarse grains, which should be quantified rather by the inter-granular void ratio than by the global void ratio. Beyond $F_c = 30\%$ the undrained shear strength at the phase transition point decreases almost linearly with increasing global void ratio (fines content) for the three densities ($D_r = 12$, 50, and 90%).

Fig. 12 shows the variation of undrained shear strength measured at the phase transition point (S_{us}) with relative density (D_r) at various fines contents. It is clear from this figure that an increase in the relative density results in an increase in the undrained shear strength at the phase transition point at a given fines content. Thevanayagam et al. [5] and Sitharam et al. [22] report a similar behaviour of increasing undrained shear strength with increasing relative density. The present laboratory study focuses on the effect of the inter-granular void ratio on the undrained shear strength of silty sands at the phase transition point at various relative densities ($D_r = 12$, 50 and 90%). The results of this study demonstrate a significant decrease in the undrained shear strength at the phase transition point with increase in the fines content or the inter-granular void ratio, but there is a significant increase in the undrained shear strength at the phase transition point with increase in the relative density and a significant decrease of the undrained shear strength at the phase transition point with the increase of the fines content. The findings of the present study is in good agreement with the experimental work reported by Ishihara [20] on Tia Juana silty sand, Baziar and Dobry [23] on silty sands retrieved from the Lower San Fernando Dam, and by Naeini and Baziar [10] on Adebil sand with different fractions of fines content.

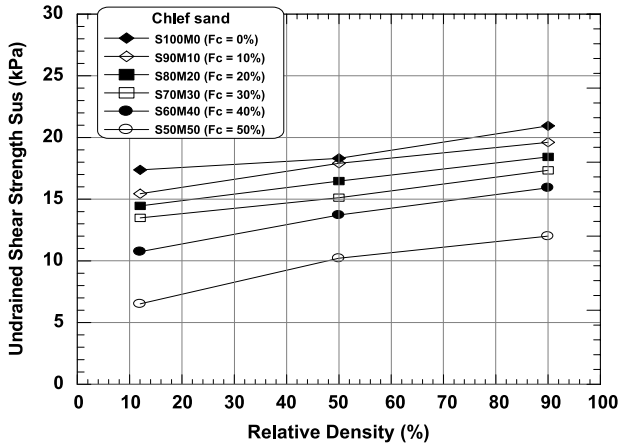

Fig. 12. Undrained shear strength at the phase transition point versus relative density and fines content ($\sigma_3' = 100$ kPa).
Fig. 12. Résistance au cisaillement en phase transitoire en fonction de la densité relative et teneur en fines ($\sigma_3' = 100$ kPa).

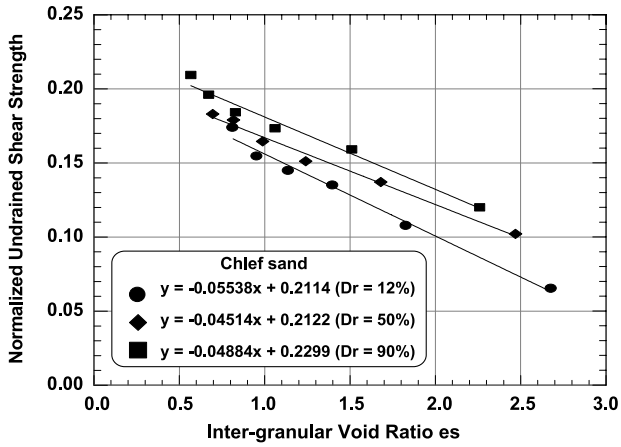

Fig. 13. Normalized undrained shear strength at the phase transition point versus inter-granular void ratio ($\sigma_3' = 100$ kPa).
Fig. 13. Résistance au cisaillement normalisée en phase de transition en fonction de l'indice des vides intergranulaire ($\sigma_3' = 100$ kPa).

Fig. 13 shows the normalized undrained shear strength measured at the phase transition point versus inter-granular void ratio. It seems that the variation of the undrained shear strength at the phase transition point due to the amount of fines, is related to the inter-granular void ratio in the range 0–50% fines content. In this case, the behaviour of silty sand samples is influenced by the contacts between coarser grains, which is quantified by the inter-granular void ratio. By increasing the fines content in the range of 0–50%, the contact between sand grains decreases and therefore the inter-granular void ratio increases and the undrained shear strength at the phase transition point decreases. Hence, in the range of 0–50% fines content, we assumed that the undrained shear strength at the phase transition point decreases linearly with the increase of the inter-granular void ratio. In this case, the following expressions are proposed to evaluate the undrained shear strength at the phase transition point which is a function of the inter-granular void ratio (e_s) and the initial effective confining pressure (σ_c') for the range of 0 to 50% fines content in normally consolidated undrained triaxial compression tests:

$$S_{us}/\sigma_c' = 0.2114 - 0.05538(e_s) \quad \text{for } D_r = 12\%$$
$$S_{us}/\sigma_c' = 0.2122 - 0.04514(e_s) \quad \text{for } D_r = 50\%$$
$$S_{us}/\sigma_c' = 0.2299 - 0.04884(e_s) \quad \text{for } D_r = 90\%$$

4. Cyclic test results

4.1. Undrained loading tests

Three series of stress-controlled cyclic triaxial tests were carried out on isotropically consolidated soil specimens with different fines content ranging from 0 to 40% and alternated symmetric deviator stress under undrained conditions to

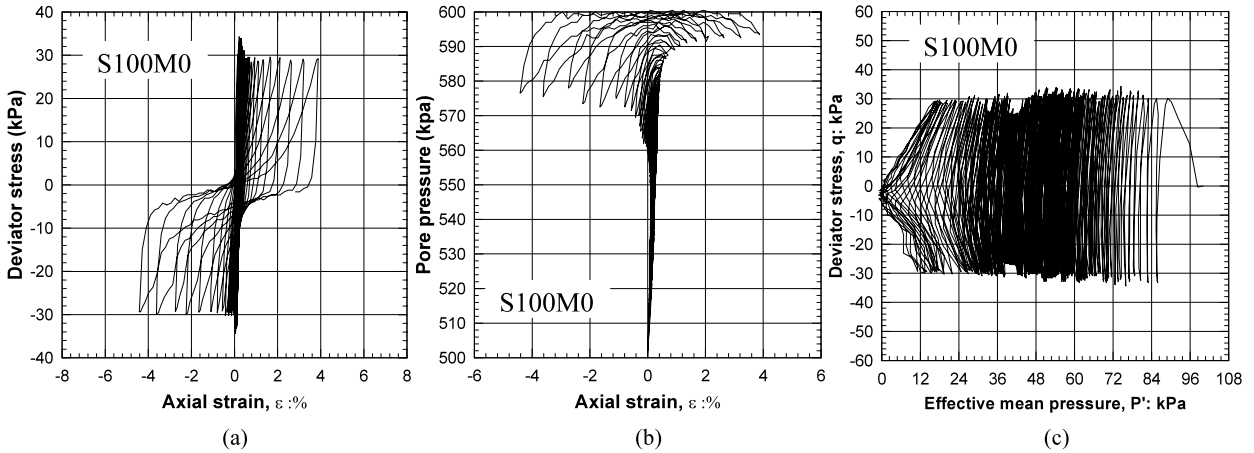

Fig. 14. Undrained cyclic response of clean sand ($F_c = 0\%$, $e_s = 0.695$, $e = 0.695$, $q_m = 30$ kPa, $D_r = 50\%$).

Fig. 14. Réponse cyclique non drainée du sable propre ($F_c = 0\%$, $e_s = 0.695$, $e = 0.695$, $q_m = 30$ kPa, $D_r = 50\%$).

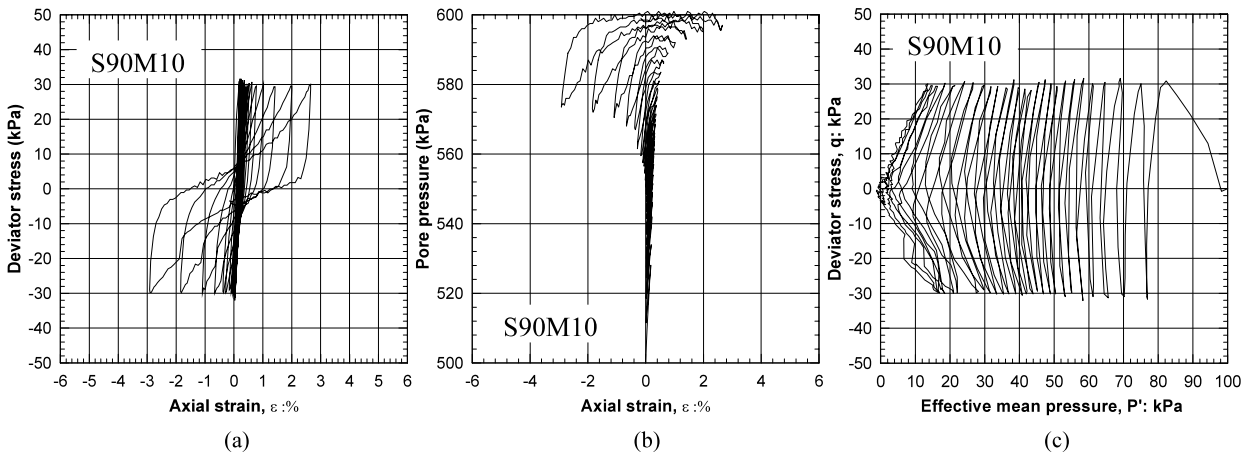

Fig. 15. Undrained cyclic response of sand–silt mixture ($F_c = 10\%$, $e_s = 0.817$, $e = 0.635$, $q_m = 30$ kPa, $D_r = 50\%$).

Fig. 15. Réponse cyclique du mélange sable–limon ($F_c = 10\%$, $e_s = 0.817$, $e = 0.635$, $q_m = 30$ kPa, $D_r = 50\%$).

simulate essentially undrained field conditions during earthquakes. In the entire test program, a frequency of 0.5 Hz was maintained. Table 2 summarizes the initial index properties of tested samples. The first series, which included three successive cyclic tests used clean sand samples ($e_s = 0.695$) with a relative density of 50% and an initial confining pressure of 100 kPa. The cycle amplitudes (q_m) were respectively 30, 50 and 70 kPa. The tests of the second series were made on the sand–silt mixture samples with an inter-granular void ratio of 0.817 and loading amplitudes of 30, 40 and 60 kPa; while the third series of tests concerned samples with an inter-granular void ratio of 1.680 and loading amplitudes of 20, 30 and 50 kPa. It was noted that the inter-granular void ratio greatly affects the liquefaction of the samples. Fig. 14 illustrates the results of the test carried out on clean sand samples ($e_s = 0.695$) with loading amplitude of 30 kPa. It is clear from the figure that the pore water pressure increases during the cycles causing a reduction of the average effective pressure. The rate of increase in the pore pressure remains low, because liquefaction is obtained only after 158 cycles (Fig. 14); for the test with $q_m = 30$ kPa and an inter-granular void ratio of 0.817 (Fig. 15), we noticed a significant increase in the pore-water pressure during the 27th cycle with a significant development of the axial strain (2.5%) leading to the liquefaction of the sample (Fig. 16).

For the test with a loading amplitude of 30 kPa and an inter-granular void ratio of 1.680, we noticed a significant increase in the pore-water pressure during the 3rd cycle with a development of the axial strain leading to the liquefaction of the sample in the 4th cycle (Fig. 17). This shows that the increase in the inter-granular void ratio in the range of (0.695–1.680) leads to an increase in the risk of liquefaction.

Fig. 16. View of liquefied silty sand sample ($e_s = 0.817$, $q_m = 30$ kPa, $D_r = 50\%$).

Fig. 16. Vue d'un échantillon de sable limoneux liquéfié ($e_s = 0.817$, $q_m = 30$ kPa, $D_r = 50\%$).

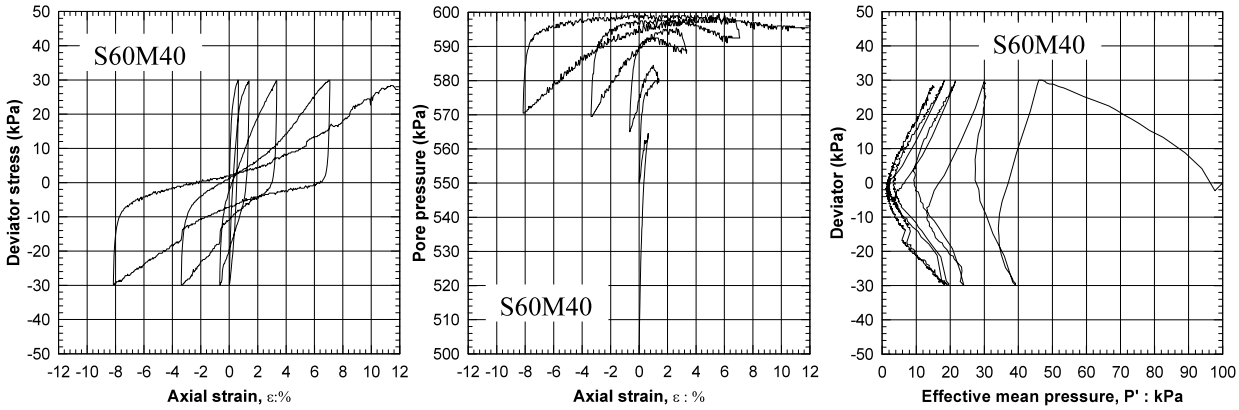

Fig. 17. Undrained cyclic response of sand–silt mixture ($F_c = 40\%$, $e_s = 1.680$, $e = 0.605$, $q_m = 30$ kPa, $D_r = 50\%$).

Fig. 17. Réponse cyclique du mélange sable–limon ($F_c = 40\%$, $e_s = 1.680$, $e = 0.605$, $q_m = 30$ kPa, $D_r = 50\%$).

4.2. Influence of the inter-granular void ratio on the liquefaction potential

Figs. 18a and 18b show the variation of the cyclic stress ratio ($\mathrm{CSR} = q_{\max}/2\sigma c'$) and the cyclic liquefaction resistance (CLR) with the number of cycles (N_c) and inter-granular void ratio (e_s) respectively. According to Ishihara [20], the cyclic liquefaction resistance (CLR) is defined as the ratio of cyclic stress leading to liquefaction for 15 cycles. We noticed that the liquefaction potential of the sand–silt mixture decreases with further increase in the inter-granular void ratio. These results confirm those found during monotonic tests showing that the increase in the inter-granular void ratio amplifies the phase of contractancy. Consequently, the amplification of the contractancy phase induces a reduction in the liquefaction potential when the inter-granular void ratio (e_s) increases. For the mixture of Chlef sand–silt, the variation of the inter-granular void ratio amplified the phase of contractancy resulting in a significant decline of the liquefaction potential. Note that for the studied amplitude ($q_m = 30$ kPa), the increase in the inter-granular void ratio in the range of 0–40% fines content leads to an acceleration of liquefaction. Fig. 18c shows the cycles of loading until liquefaction versus the inter-granular void ratio. We observed that the liquefaction resistance decreases with the increase of the inter-granular void ratio. The samples sheared with higher level loading ($\mathrm{CSR} = 0.25$) are more vulnerable to liquefaction than those sheared with smaller loading level ($\mathrm{CSR} = 0.15$).

4.3. Effect of the relative density

Undrained cyclic tests were performed on Chlef sand–silt mixtures ($F_c = 5\%$) for three relative densities ($D_r = 12$, 45 and 60%). For each density, we varied the loading amplitude in order to draw the liquefaction potential curve. The tests were carried out for the amplitudes $q_m = 30$, 50 and 70 kPa. Liquefaction was reached quickly for the higher amplitudes: after

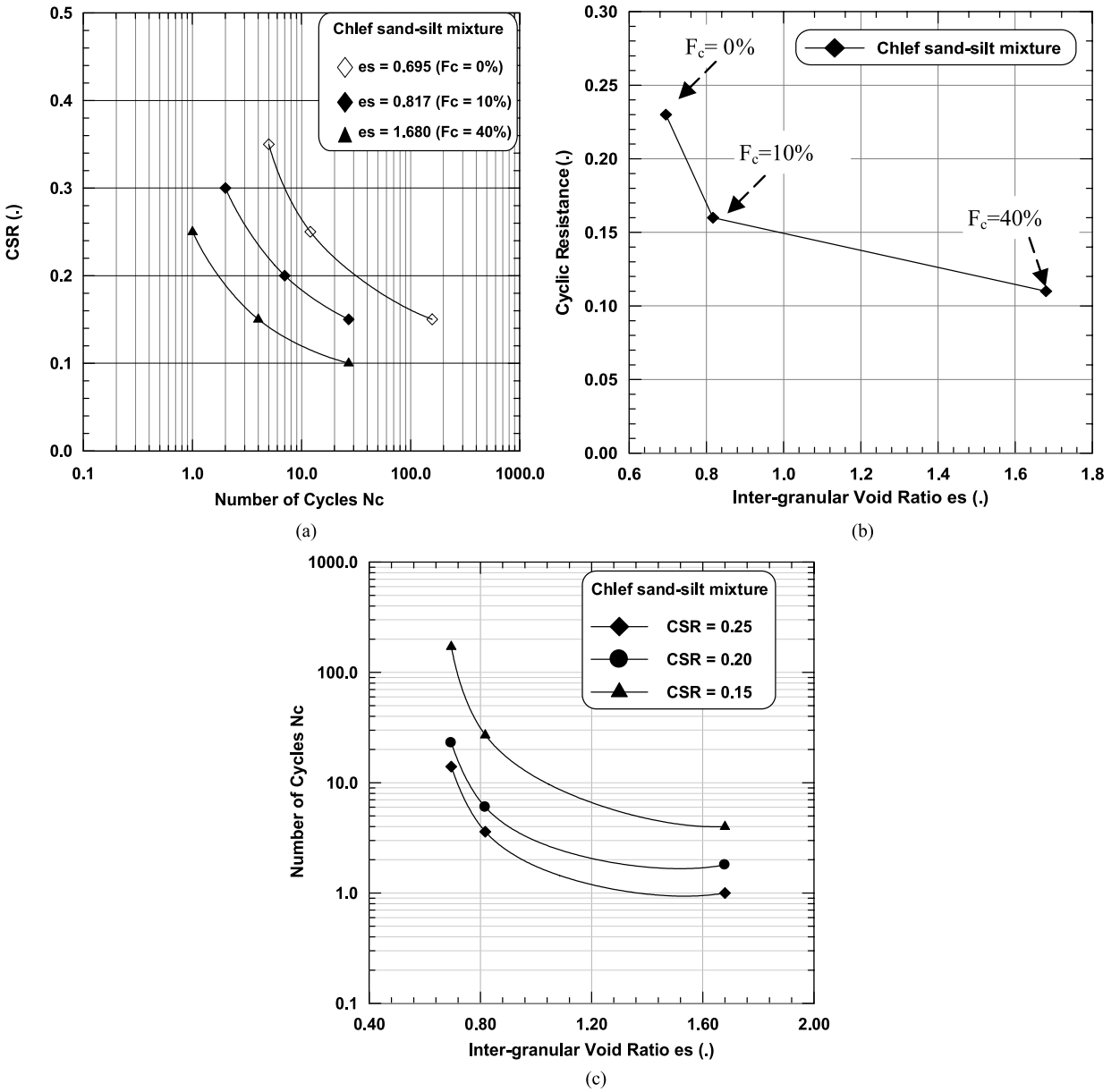

Fig. 18. Inter-granular void ratio effect on the liquefaction potential of the Chlef sand–silt mixtures ($\sigma'_3 = 100$ kPa, $D_r = 50\%$).

Fig. 18. Effet de l'indice des vides intergranulaire sur le potentiel de liquéfaction des mélanges sable–limon ($\sigma'_3 = 100$ kPa, $D_r = 50\%$).

two and three cycles respectively for loading amplitudes of $q_m = 70$ and 50 kPa, whereas the liquefaction under the loading amplitude of $q_m = 30$ kPa for the tests carried out with a relative density $D_r = 12\%$ was reached at 24 cycles; for the same loading amplitudes, liquefaction was obtained only after 4, 5 and 71 cycles for the tests with a relative density of $D_r = 45\%$. For the tests carried out with a relative density of $D_r = 60\%$ and for the same loading amplitudes, liquefaction was reached at 5, 13 and 167 cycles.

Fig. 19 summarizes the results of all these tests. Fig. 19a illustrates the influence of the relative densities ($D_r = 12$, 45 and 60%) on the liquefaction potential of the Chlef sand–silt mixture ($F_c = 5\%$). It shows clearly that the increase in the relative density leads to an increase in the liquefaction resistance of the Chlef sand–silt mixture. Fig. 19b shows the influence of the inter-granular void ratio on the liquefaction resistance defined by the amplitude of the loading inducing liquefaction after 15 cycles for the Chlef sand–silt mixture. This figure shows clearly that the liquefaction resistance decreases with the increase in the inter-granular void ratio and the loading amplitude. We note that the reduction in the liquefaction resistance of Chlef sand–silt mixture becomes very marked for the smaller cyclic stress ratios CSR = 0.15 and 0.25.

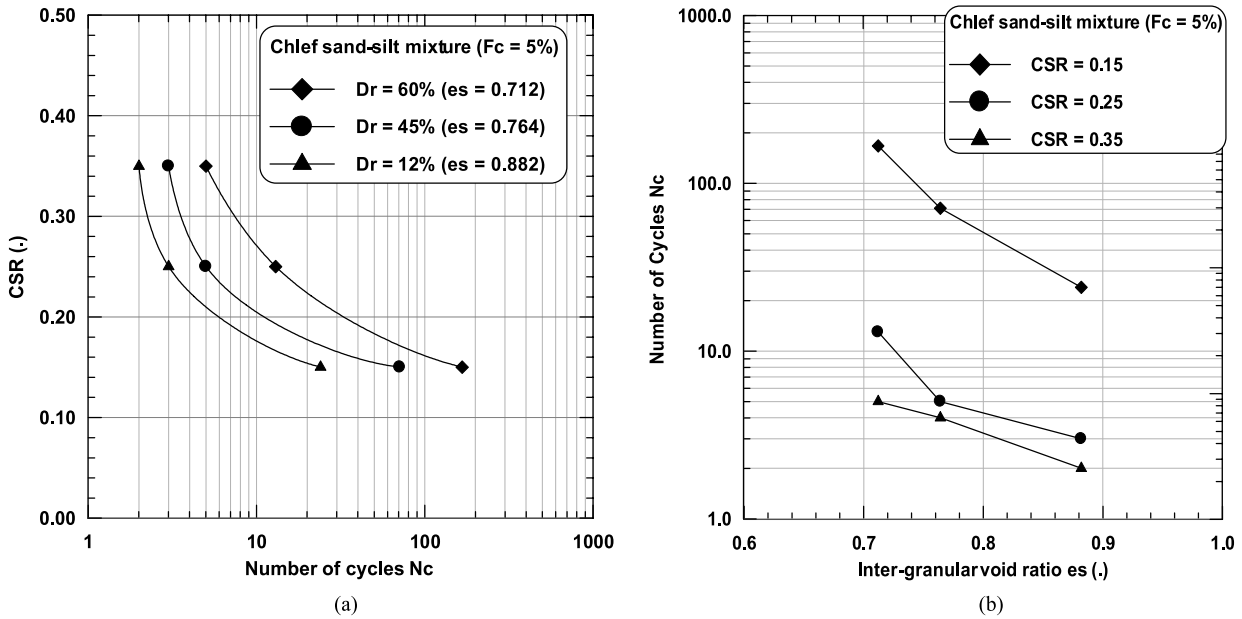

Fig. 19. Relative density effect on the liquefaction potential of the Chlef sand–silt mixture ($\sigma'_3 = 100$ kPa, $F_c = 5\%$).

Fig. 19. Effet de la densité relative sur le potentiel de liquéfaction du mélange sable–limon ($\sigma'_3 = 100$ kPa, $F_c = 5\%$).

5. Conclusion

The effect of the inter-granular void ratio on the undrained shear strength at the phase transition state and the liquefaction potential of sand–silt mixtures was investigated in the present laboratory study. In the light of the experimental evidence, the following conclusions can be drawn:

The results of different triaxial tests on loose, medium dense and dense silty sands show clearly that there is a correlation between the undrained shear strength measured at the phase transition point (S_{us}) and the inter-granular void ratio (e_s), which is the void ratio of the sand-grain matrix. It is shown that for the range 0–50% of the fines content, the undrained shear strength at the phase transition state decreases linearly with an increase of the inter-granular void ratio. In fact, when we increase the fines content in the range of 0–40%, all the fine-grained soil fills most of the voids in the sand-grain matrix and the contact between sand grains decreases and thus the inter-granular void ratio increases. As the fines content increases the undrained shear strength at the phase transition state decreases until a fines content of 40% is reached. After that a strong decline in the undrained shear strength at the phase transition point was observed.

Undrained cyclic tests show that the liquefaction potential of the sand–silt mixture decreases with further increases in the inter-granular void ratio (fines content) and the samples sheared with higher level loading (CSR = 0.25) are more vulnerable to liquefaction than those sheared with a lower loading level (CSR = 0.15). They also show that the liquefaction resistance increases with the relative density but it decreases with the increase in the inter-granular void ratio and the loading amplitude. The reduction in the liquefaction resistance of the Chlef sand–silt mixture becomes very marked for the smaller cyclic stress ratios CSR = 0.15 and 0.25.

These results confirm those found during monotonic tests showing that the increase in the inter-granular void ratio amplifies the phase of contractancy inducing a reduction in the liquefaction potential when the inter-granular void ratio increases. For the Chlef sand–silt mixtures, the inter-granular void ratio amplifies the phase of contractancy resulting in a significant decline of the liquefaction potential. Note that for the studied amplitude ($q_m = 30$ kPa), the increase in the inter-granular void ratio ($e_s = 0.695$ to 1.680) in the range of 0–40% fines content leads to an acceleration of liquefaction.

References

[1] S. Thevanayagam, Dielectric dispersion of porous media as a fractal phenomenon, J. Appl. Phys. 82 (5) (1997) 2538–2547.
[2] S. Thevanayagam, S. Nesarajah, Fractal model for flow through saturated soil, J. Geotech. Geoenviron. Eng., ASCE 124 (1) (1998) 53–66.
[3] S. Zlatovic, K. Ishihara, On the influence of non-plastic fines on residual strength, in: Proc. of the First Int. Conf. on Earthquake Geotech. Eng., Tokyo, 1995, pp. 14–16.
[4] P.V. Lade, J.A. Yamamuro, Effects of non-plastic fines on static liquefaction of sands, Canadian Geotech. J. 34 (1997) 918–928.
[5] S. Thevanayagam, K. Ravishankar, S. Mohan, Effects of fines on monotonic undrained shear strength of sandy soils, ASTM Geotech Testing J. 20 (1) (1997) 394–406.
[6] S. Thevanayagam, Effect of fines and confining stress on undrained shear strength of silty sands, J. Geotech. Geoenviron. Eng., ASCE 124 (6) (1998) 479–491.
[7] J.A. Yamamuro, P.V. Lade, Steady-state concepts and static liquefaction of silty sands, J. Geotech. Geoenviron. Eng., ASCE 124 (9) (1998) 868–877.

[8] F. Amini, G.Z. Qi, Liquefaction testing of stratified silty sands, J. Geotech. Geoenviron. Eng., ASCE 126 (3) (2000) 208–217.
[9] S.A. Naeini, The influence of silt presence and sample preparation on liquefaction potential of silty sands, PhD dissertation, Iran University of Science and Technology, Tehran, 2001.
[10] S.A. Naeini, M.H. Baziar, Effect of fines content on steady-state strength of mixed and layered samples of a sand, Soil Dynam. Earth. Eng. 24 (2004) 181–187.
[11] J. Chu, W.K. Leong, Effect of fines on instability behaviour of loose sand, Geotechnique 52 (10) (2002) 751–755.
[12] M.M. Monkul, Influence of inter-granular void ratio on one dimensional compression, M.Sc. thesis, Dokuz Eylul University, Izmir, Turkey, 2005.
[13] R.S. Ladd, Preparing test specimen using under compaction, Geotech. Testing J., GTJODJ 1 (1978) 16–23.
[14] T.C. Kenny, Residual strengths of mineral mixtures, in: Proc. 9th Int. Conf. Soil Mech. and Found. Eng., Tokyo, vol. 1, 1977, pp. 155–160.
[15] R. Kuerbis, D. Nagussey, Y.P. Vaid, Effect of gradation and fines content on the undrained response of sand, in: Proc. Hyd. Fill. Struc. Geotech. Spec. Publ., vol. 21, ASCE, New York, 1988, pp. 330–345.
[16] J.K. Mitchell, Fundamental of Soil Behaviour, 2nd ed., John Wiley–Interscience, New York, 1993.
[17] S. Thevanayagam, S. Mohan, Inter-granular state variables and stress-strain behaviour of silty sands, Geotechnique 50 (1) (2000) 1–23.
[18] C.K. Shen, J.L. Vrymoed, C.K. Uyeno, The effects of fines on liquefaction of sands, in: Proc. 9th Int. Conf. Soil Mech. and Found. Eng., Tokyo, vol. 2, 1977, pp. 381–385.
[19] J.H. Troncosco, R. Verdugo, Silt content and dynamic behaviour of tailing sands, in: Proc. 12th Int. Conf. on Soil Mech. and Found. Eng., San Francisco, 1985, pp. 1311–1314.
[20] K. Ishihara, Liquefaction and flow failure during earthquakes, Geotechnique 43 (3) (1993) 351–415.
[21] M.P. Luong, Etat caractéristique du sol, C. R. Acad. Sci. Paris Ser. B 287 (1978) 305–307.
[22] T.G. Sitharam, L. Govinda Raju, B.R. Srinivasa Murthy, Cyclic and monotonic undrained shear response of silty sand from Bhuj region in India, ISET J. Earthquake Technol. 41 (2–4) (June–December 2004) 249–260.
[23] M.H. Baziar, R. Dobry, Residual strength and large-deformation potential of loose silty sands, J. Geotech. Eng., ASCE 121 (1995) 896–906.